Accepted Manuscript

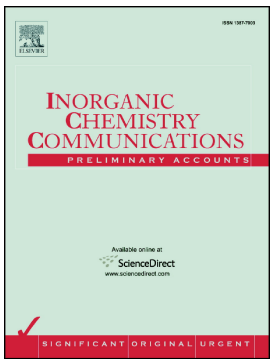

Thiophene and furan appended pyrazoline based fluorescent chemosensors for detection of Al3+ ion

Rangasamy Manjunath, Palaninathan Kannan

PII: S1387-7003(18)31042-6
DOI: https://doi.org/10.1016/j.inoche.2019.01.038
Reference: INOCHE 7254

To appear in: *Inorganic Chemistry Communications*

Received date: 27 November 2018
Revised date: 24 January 2019
Accepted date: 25 January 2019

Please cite this article as: R. Manjunath and P. Kannan, Thiophene and furan appended pyrazoline based fluorescent chemosensors for detection of Al3+ ion, Inorganic Chemistry Communications, https://doi.org/10.1016/j.inoche.2019.01.038

Thiophene and furan appended pyrazoline based fluorescent chemosensors for detection of Al^{3+} ion

Rangasamy Manjunath and Palaninathan Kannan*

Department of Chemistry, Anna University, Chennai - 600 025, India.

Abstract

Thiophene and furan appended pyrazoline receptors R1 and R2 were designed and synthesized for selective detection of Al^{3+} ion. Their photophysical properties were studied by UV-visible and fluorescence spectra. Surprisingly, both receptors R1 and R2 were displayed an excellent selective and sensitive response to Al^{3+} ion alone over other tested metal ions. Both the receptor R1 and R2 displays 1:1 stoichiometry for [R1-Al^{3+}] and [R2-Al^{3+}] complex and formed with an association constant of 1.84×10^4 M^{-1} and 1.92×10^4 M^{-1} respectively. The limit of detection were calculated for R1 and R2 since 8.92×10^{-8} M and 1.04×10^{-7} M by the fluorescence titration method. The thiophene based receptor R1 exhibited superior chemosensor characteristics such as high intensity absorption and emission at longer wavelength as compered that of furan based receptor R2.

Keywords: Pyrazoline; Thiophene; Furan; Chemosensor; Aluminum (III) ion;

Corresponding author: Dr. P. Kannan

E-mail: pakannan@annauniv.edu , Tel: +91 44 2235 8666, Fax: +91 44 2220 0660

Introduction

The design and synthesis of highly selective and sensitive fluorescent chemosensor for detection of heavy and transition metals ions is still a hot research area in chemistry, biochemistry, biology, material science and environmental science [1-6]. These metal ions are entered into environment through natural and anthropogenic activities and biologically and environmentally-important species. The presence of these metal ions is critical for human life, ascribed to their toxicity.

The trivalent cation found in its ionic form in most kind of animals, plant tissues and in natural waters everywhere [7,8]. Aluminum is the third most abundant element in the earth's crust and its compounds comprise about 8.8% by weight of the Earth's surface[9]. People are widely exposed to aluminum attributed to its widespread use in food additives, pharmaceuticals, and cooking utensils, aluminum foil, vessels, trays and cosmetics [10,11].

Excessive exposure of human body to Al^{3+} ion can be more toxic to human health[12]. The excess aluminum can cause damages to certain human tissues and cells, resulting Alzheimer's disease and Parkinson's disease, aluminum accumulation in the body leading to bone and brain damage [13-17]. Additionally, the concentration of aluminum has been found to be crucial for fish, and also for agricultural production as it increases acidity of the soil. Aluminum is toxic to plants at micro molar concentration, the phytotoxicity of aluminum is rapid inhibition of root elongation of the plant, and aluminum may interact with root cell walls, disrupt plasma membrane and inhibit transport process on the plasma membrane[18].

A variety of analytical methods are available for determination of Al^{3+} ion, including, photometric methods, flame or graphite furnace, atomic absorption spectroscopy (AAS), inductively coupled plasma emission or mass spectrometry (ICP-ES, ICP-MS), anodic

stripping voltammetry (ASV), atomic emission spectrometry, etc are available for detection of Al^{3+} ion [19–22]. But these methods require sophisticated analytical instruments. On the other hand, the fluorescence detection method has concerned significant attention attributed to its high signaling ability along with high sensitivity and selectivity, enable on-line and field monitoring. Thus, emerged as useful alternative tool [23, 24].

Herein, we report the synthesis of thiophene and furan appended pyrazoline derivatives R1 and R2. Both the receptors displayed an excellent selective and sensitive response to Al^{3+} ion over other tested metal ions.

Experimental

Materials and Instruments

Deionized water was used throughout the experiment. All the chemicals for synthesis were purchased from commercial suppliers and used after further purification. Perchlorate salts of Na^{+}, Mg^{2+}, Al^{3+} K^{+}, Ca^{2+}, Mn^{2+}, Fe^{3+}, Co^{2+}, Ni^{2+}, Cu^{2+}, Zn^{2+}, Cd^{2+} and Hg^{2+} were purchased from Alfa Aesar, India. All the reagent-grade solvents were purified according to the standard procedures and freshly distilled prior to use [25]. All the synthesis was monitored by thin layer chromatography with detection by UV. Thin layer chromatography (TLC) was performed on silica gel 60 F_{254} plates (Merck KGaA). Column chromatography was executed on silica gel (60–120 mesh). FT-IR spectra were recorded with IR spectrometer Perkin-Elmer FT-IR spectrometer using KBr pellets. ^{1}H-NMR spectra were recorded on Bruker AVIII 300 MHz spectrometer using tetramethylsilane (TMS) as an internal reference. Electron spray mass spectra (ESI-MS) were carried out on a Bruker MaXis 10138 HRMS instrument. UV-vis spectra were recorded in room temperature using a Shimadzu UV-

1650PC spectrophotometer. Fluorescence spectra were recorded in room temperature using Perkin Elmer LS-45 Fluorescence spectrophotometer.

Synthesis of receptor R1 and R2

The synthetic route of the prepared receptors R1 and R2 is depicted in Scheme 1. (E)-3-(3-hydroxyphenyl)-1-(thiophen-2-yl)prop-2-en-1-one and (E)-1-(furan-2-yl)-3-(3-hydroxy phenyl)prop-2-en-1-one were prepared according to the literature procedures[26- 27]. To a stirred solution of chalcones (**2**) and (**3**), (1.0 mmol) and NaOH (3 mmol) in ethanol (15 mL) 2-hydrazinobenzothiazole (1.0 mmol) was added and reaction mixture were refluxed for 6 h respectively. The progress of the reaction was monitored by TLC. After completion, the reaction mixture was cooled to room temperature, resultant mixture quenched with ice water and solution neutralized with dilute hydrochloric acid. The crude products were obtained as pale yellow precipitate, filtered, washed with water and ethanol and recrystallized with ethanol to give products with 80% yield. 3-(1-(benzo[d]thiazol-2-yl)-3-(thiophen-2-yl)-4,5-dihydro-1H-pyrazol-5-yl)phenol (R1) IR (Fig.S5) (γ_{max}, KBr, cm^{-1}): 3437, 1600, 1532,1450,1236, 705; ^{1}H NMR (Fig. S1) (300 MHz, $CDCl_3$) δ (ppm): 10.01 (s, 1H), 7.82 (s, 1H),7.65 (s, 1H),7.43 (d, 2H), 6.97 (s, 1H),6.94 – 6.90 (m, 3H),6.85 (d, 2H),6.75 – 6.63 (s, 1H), 5.79 (s, H), 3.88 (s, 1H), 3.23 (s, 1H).; ^{13}C NMR (Fig. S3) (100 MHz, DMSO–d_6): δ 165.01, 156.46, 154.80, 152.00, 140.92, 138.35, 134.57, 130.60, 129.27, 127.37, 127.11, 126.08, 122.63, 122.41, 119.55, 119.22, 116.36, 116.21, 77.28, 77.03, 76.77, 67.15, 39.84.; MS (ESI^+): m/z (%): 377.48(100) $(M + H)^+$ (Fig. S6)

3-(1-(benzo[d]thiazol-2-yl)-3-(furan-2-yl)-4,5-dihydro-1H-pyrazol-5-yl)phenol(R2) IR (Fig. S5) (γ_{max}, KBr, cm^{-1}): 3427, 1606, 1532, 1456, 1242, 758; ^{1}H NMR (Fig. S2) (300 MHz,

$CDCl_3$) δ (ppm): 10.01 (s), 7.62 (s, 1H),7.59 (s, 1H),7.26 (s, 1H), 7.17 (d, J = 3.1 Hz, 2H) 7.05(s, 1H),6.81 (d, J = 11.6 Hz, 2H),6.68(s, 1H),6.59 (s, 1H), 6.54 (s, 1H), 5.95 (s, 1H), 3.88 (s, 1H), 3.26 (s, 1H).; ^{13}C NMR (Fig. S4) (100 MHz, DMSO–d_6): δ 165.01, 156.46, 154.80, 152.00, 140.92, 138.35, 134.57, 130.60, 129.27, 127.37, 127.11, 126.08, 122.63, 122.41, 119.55, 119.22, 116.36, 116.21, 77.28, 77.03, 76.77, 67.15, 39.84.; MS (ESI^+): m/z (%): 361.42 (100) $(M + H)^+$ (Fig. S7).

General procedure for spectral detection

The stock solutions of R1 and R2 (1.0 $x10^{-5}$ M) were prepared by dissolving in acetonitrile. The cationic stocks were all dissolved in deionized water with concentration of 10^{-3} M for UV–Vis absorption and fluorescence spectral analysis. UV-visible and fluorescence titration experiments were performed using 1.0 × 10^{-5}M and 10^{-5}M of R1 and R2 in HEPES buffer (20 mM HEPES, pH = 7.2, 50% (v/v) CH_3CN), respectively. The sensing studies were carried out by monitoring absorption and fluorescence spectral analyses, 3 mL solution of R1 and R2 were filled in a quartz cell of 1 cm optical path length, and gradually increased Al^{3+} ion concentration using a micro-pipette every time. They were kept 1 min for incubation after each addition of Al^{3+} ion.

Job's plot analyses

The stoichiometric behavior of receptors R1 and R2 towards Al^{3+} ion were determined by Job's plot method using fluorescence titration data [28]. The total concentration of receptor and Al^{3+} ion kept as constant and mole fraction of Al^{3+} ion altering from 0 to 1. Fluorescence spectra were recorded for all portions. The relative fluorescence intensity values was plotted against $[Al^{3+}]/ \{[Al^{3+}]+[\mathbf{R}]\}$. The mole fraction of Al^{3+} at which the emission intensity is at maximum gives the stoichiometry of complex from the plot.

Determination of association constant

The association constant can be estimated by fluorescence titration according to Benesi-Hildebrand equation [29]

$$\frac{1}{(\Delta F)} = \frac{1}{K_a(\Delta F_{sat})[Al^{3+}]} + \frac{1}{\Delta F_{sat}}$$

ΔF is the fluorescence difference between the presence and absence of Al^{3+} with receptor, F_{sat} is fluorescence difference at saturated, *K*a is association constant and was determined from slope of linear plot, $[Al^{3+}]$ is concentration of Al^{3+} ion added during titration studies. The goodness of linear fit of B-H plot of $1/\Delta F$ verses $1/[Al^{3+}]$ for 1:1 complex formation confirms binding stoichiometry between receptor and Al^{3+}.

Determination of quantum yield

Fluorescence quantum yield was determined using quinine sulfate dehydrate (≥ 99.0 %) in 0.1 N H_2SO_4 as the main standard. The corrected emission spectra were measured for quinine sulfate dehydrate standard (λex=330 nm; A (Absorption) <0.01; ΦF= 0.560). The general equation used in determination of relative quantum yield of samples was determined according to the following equation. [30]

$$\emptyset u = \emptyset s . \frac{Fu}{Fs} . \frac{As}{Au} . \frac{(\eta u)^2}{((\eta s)^2}$$

Where Φ*u* and Φ*s* are fluorescence quantum yield of sample and standard, *F*u and *F*s are the integrated fluorescence intensities of sample and standard, *A*u and *A*s are absorbance of sample and standard and *ηu* and *ηs* are refractive index of sample and standard solutions respectively.

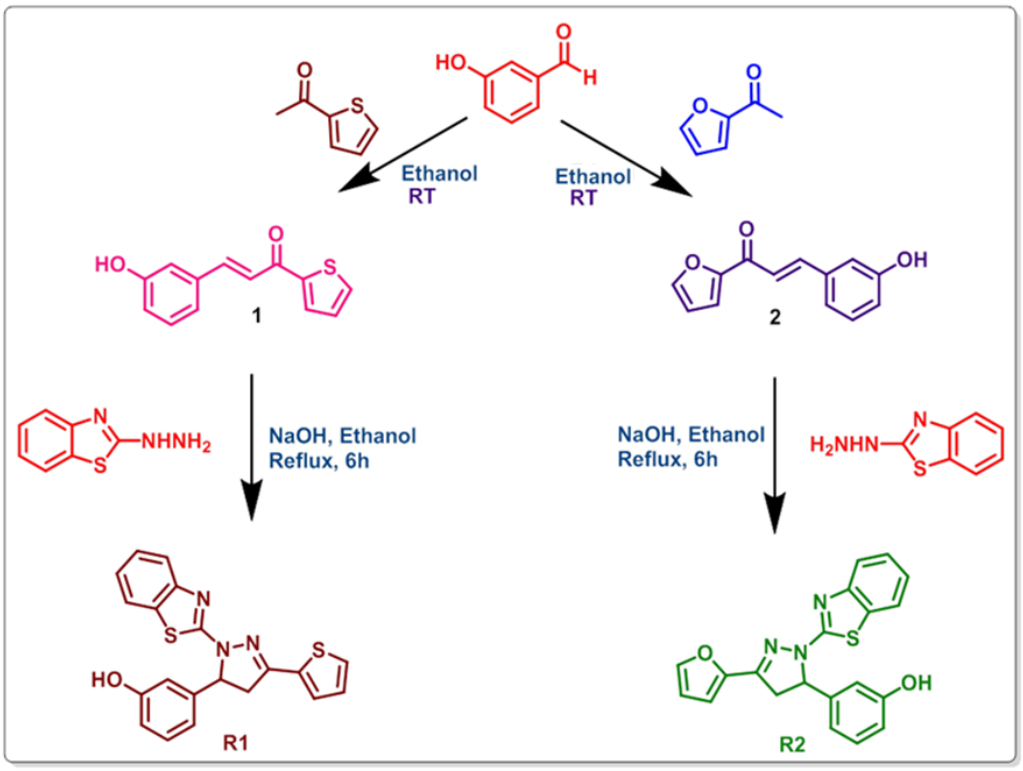

Scheme1. Synthesis of R1 and R2.

Results and discussion

The receptors R1 and R2 were facile synthesized by the reaction of chalcone **1** and **2** with 2-hydrazinobenzothiazole in ethanol under reflux in 80% yield (Scheme 1). The structure of R1 and R2 was confirmed by ^{1}H-NMR, ^{13}C-NMR and ESI-MS spectra.

Absorption and emission behavior of R1 and R2

The receptors R1 and R2 exhibits a broad absorption bond at 358 nm and 347 nm respectively (Fig.1), which could be assigned to an allowed π-π* transition and intra charge transfer (ICT) of conjugated localized pyrazoline ring system, The emission spectra of receptors R1 and R2 are depicted in Fig.2. Receptor R1 and R2 exhibited a bright blue emission with peak at 447 nm and 436 nm as similar to pyrazoline family [31, 32]. Thiophene and furan substituents present in the pyrazoline displays different emission peak range.

Among the two receptors, thiophene appended receptor R1 exhibit better photophysical properties compared to furan appended receptor R2. It reveals that pyrazoline derivatives could exhibit different emission with respect to changing substitution in pyrazoline structure.

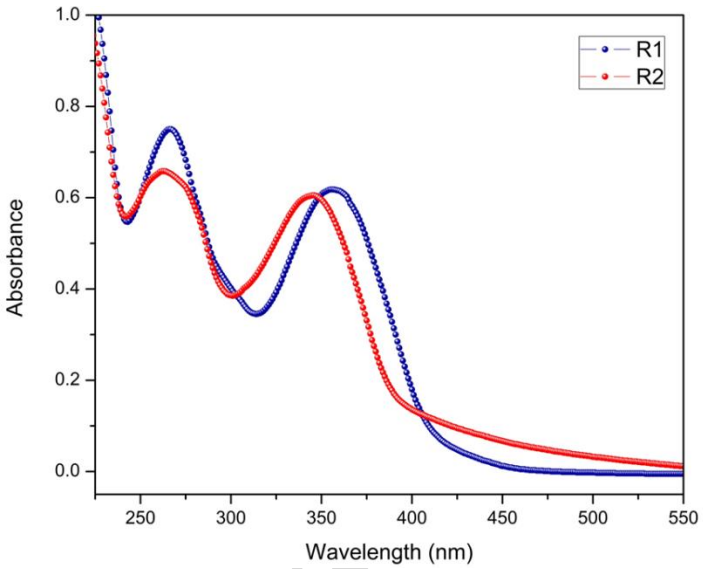

Fig. 1. UV-Vis absorption spectra of R1 and R2

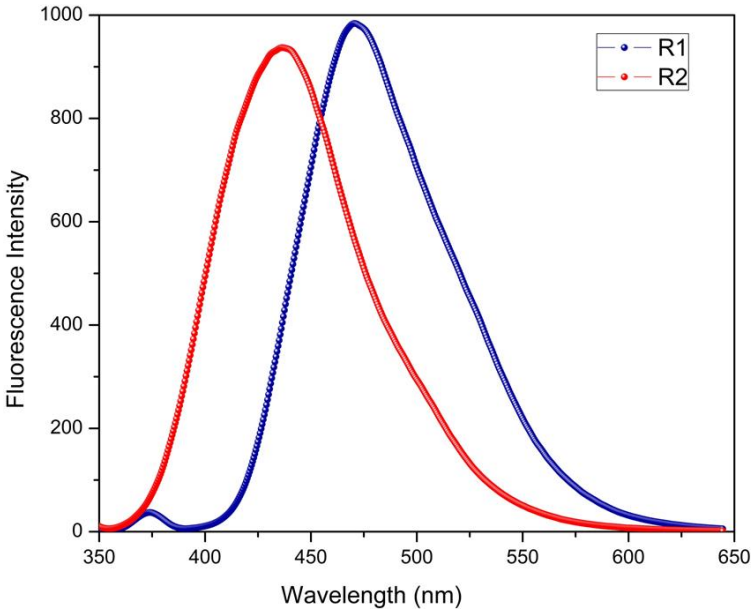

Fig. 2. Fluorescence spectra of R1 and R2

UV–Vis absorption spectral responses of R1 and R2 towards metal ions

Binding affinity of receptor R1 and R2 towards various metal ions was estimated by UV–Vis spectroscopy measurements. Addition of various metal ions to the solution of R1 and R2, absorption spectrum changes differently as evidenced in Fig. 3 and 4. In the case of Na^{+}, Mg^{2+}, K^{+}, Mn^{2+}, Fe^{3+}, Ni^{2+}, Cu^{2+}, Zn^{2+}, Cd^{2+}, Pb^{2+} and Hg^{2+} additions, there is no significant change was observed in absorption spectra of R1 and R2, whereas in the presence of Al^{3+} ion the wavelength absorption peak of R1 and R2 at 358 nm and 347 nm was shifts hypsochromically to 349 nm and 341 nm, respectively, attributed to the formation of new complex between receptor and Al^{3+} ion.

To determine the binding behavior of receptor R1 and R2 towards Al^{3+} ion, the UV-Vis absorption titration experiments were carried out in HEPES buffer solution (20 mM HEPES, pH = 7.2, 50% (v/v) (CH_3CN; Fig.S8 and S9). The progressive addition of Al^{3+}ion to solution of receptor R1 resulted in blue shift in absorption spectra, the absorption peak at 358 nm gradually hypsochromically shifted to 349 nm and its intensity gradually increased with increasing concentration of Al^{3+} ion, the absorption intensity at 266 nm was gradually decreased with isobestic point at 328 nm was ascribed to equilibrium between receptor R1 and Al^{3+} throughout the titration process, similarly addition of Al^{3+} ion to solution of receptor R2, absorbance peak at 347nm gradually blue shifted to 341 nm. This absorption peak is presumably attributed to coordination of receptor R2 with Al^{3+}ion.

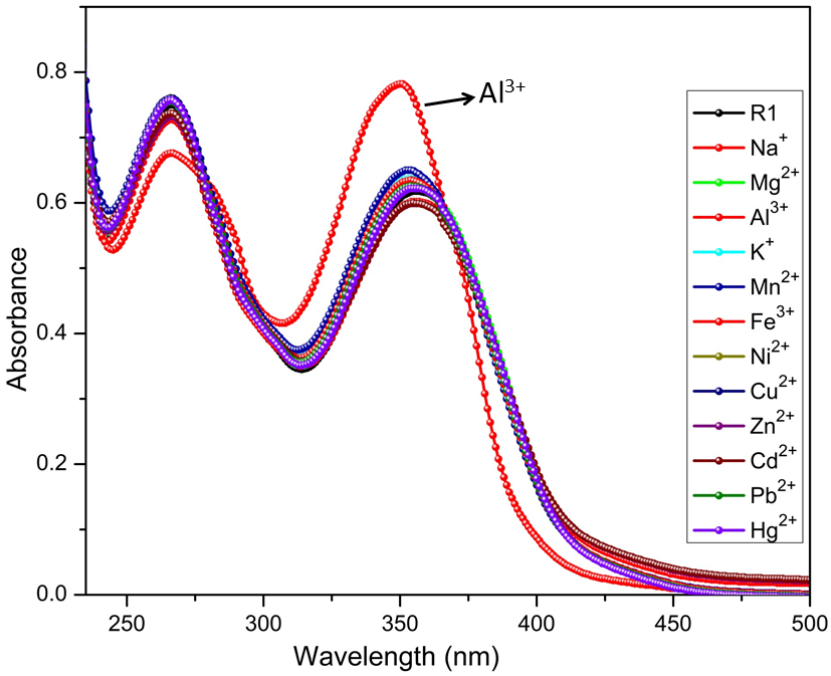

Fig.3. UV–Vis absorption spectra of R1 (1 ×10^{-5} M) in HEPES buffer solution (20 mM HEPES), pH = 7.2, 50% (v/v; CH_3CN) in the presence of various metal ions (3 × 10^{-5} M)

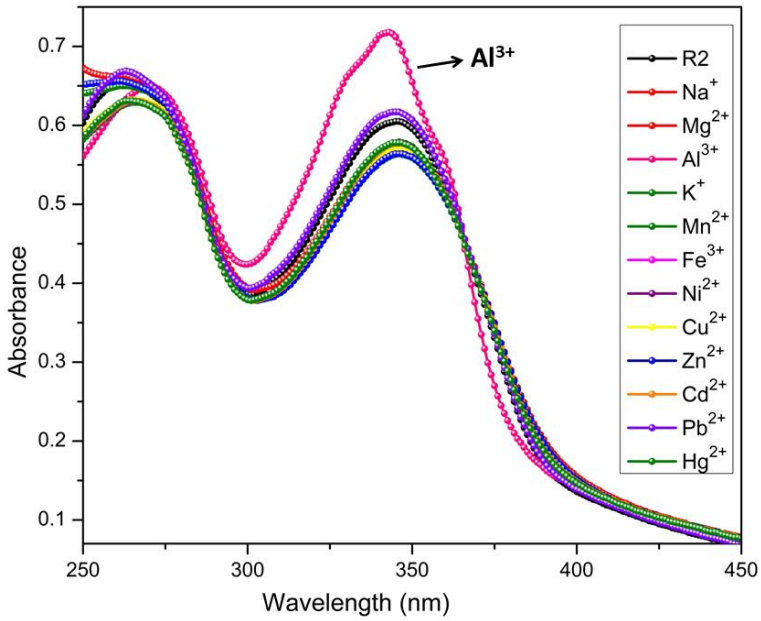

Fig.4. UV–Vis absorption spectra of R2 (1 ×10^{-5} M) in HEPES buffer solution (20 mM HEPES), pH = 7.2, 50% (v/v; CH_3CN) in presence of various metal ions (3 × 10^{-5} M)

Fluorescence spectral responses of R1 and R2 towards metal ions

The fluorescence spectrum changes of receptor R1 and R2 in HEPES buffer solution (20 mM HEPES, pH = 7.2, 50% (v/v; CH_3CN), before and after addition of different metal ions were recorded to examine the selectivity. The free receptors R1 and R2 exhibited a strong fluorescence emission at 447nm and 436nm respectively in the absence of various metal ions as depicted in Fig. 5 and 6. Interestingly, addition of 3 equiv. of various metal ions (Na^+, Mg^{2+}, Al^{3+} , K^+, Mn^{2+}, Fe^{3+}, Ni^{2+}, Cu^{2+}, Zn^{2+}, Cd^{2+}, Pb^{2+} and Hg^{2+}) to the solution of receptor R1 and R2, Al^{3+} ion alone induced remarkable quenching of fluorescence intensity at 447nm and 436nm respectively and other tested metal ions did not exhibit any significant change in emission, which reveals that receptor R1 and R2 has a high selectivity towards Al^{3+} ion.

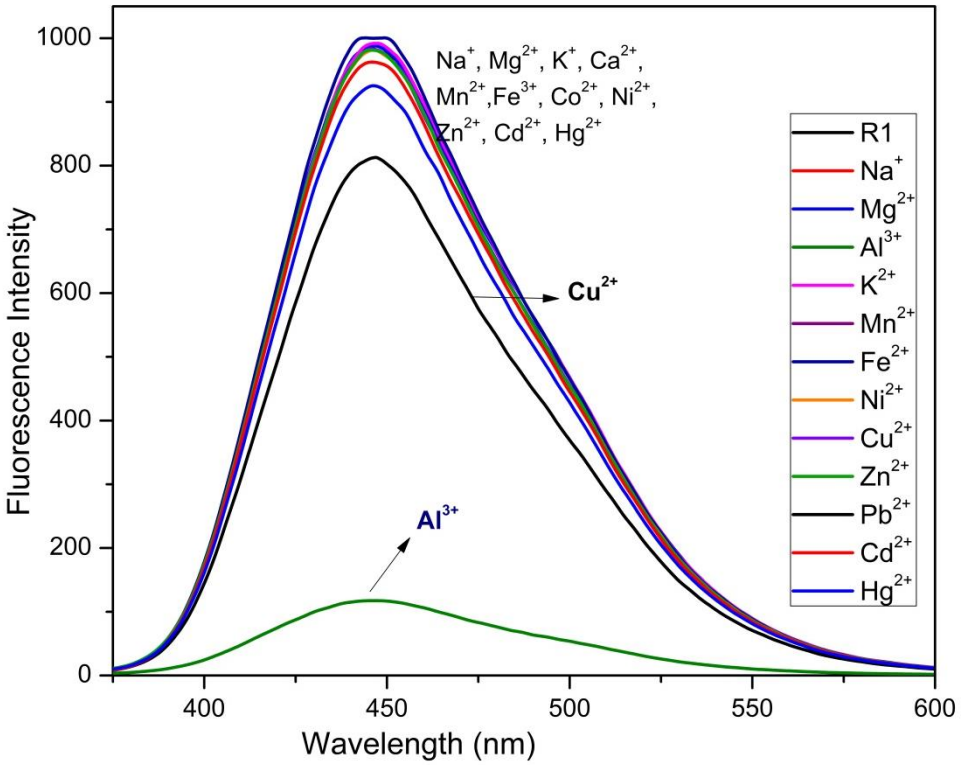

Fig. 5. Fluorescence spectra of R1 (1×10^{-5} M) in HEPES buffer solution (20 mM HEPES), pH = 7.2, 50% (v/v; CH_3CN) upon additions of various metal ions (3×10^{-5} M)

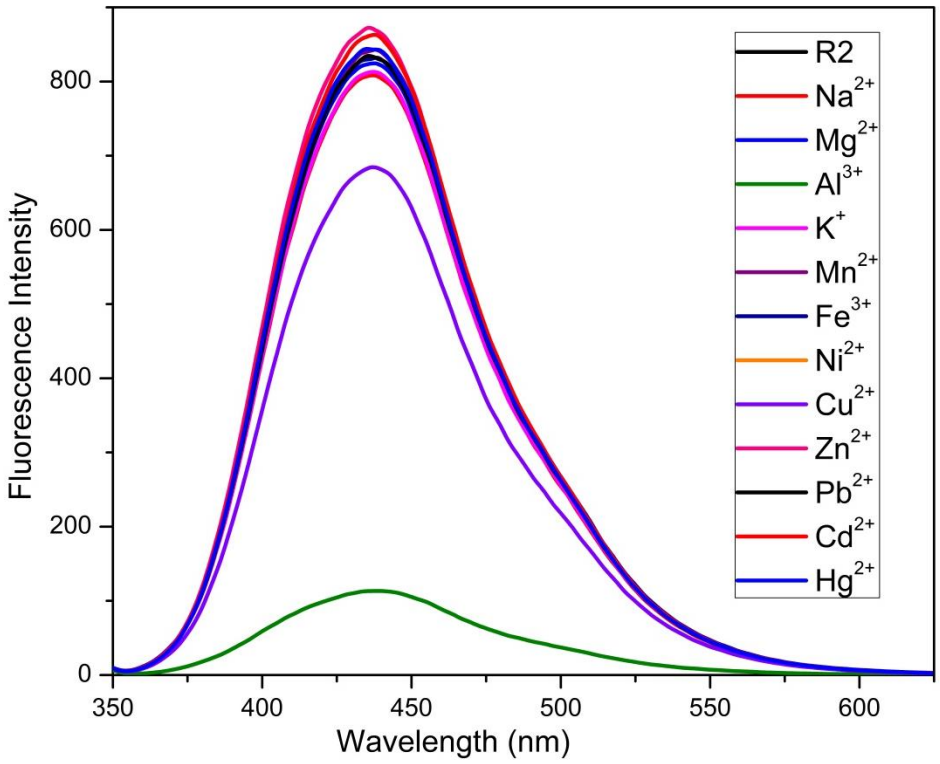

Fig. 6. Fluorescence spectra of R2 (1×10^{-5} M) in HEPES buffer solution (20 mM HEPES), pH = 7.2, 50% (v/v; CH_3CN) upon additions of various metal ions (3×10^{-5} M)

To further investigate the interaction of receptor R1 and R2 towards Al^{3+} ion, a fluorescence titration experiment was carried out, as presented in Fig. 7 and Fig.8. The free receptor R1 and R2 exhibits emission peak centered at 447nm and 436nm respectively. The fluorescence quantum yield of receptor R1 and R2 in the absence of Al^{3+} were calculated to be 0.50 and 0.47 with respect to quinine sulphate in 0.1 N H_2SO_4 solution ($\emptyset s$ = 0.54). The fluorescence intensity of receptors R1 and R2 was linearly decreased with incremental addition of Al^{3+} ion, it was quenched almost completely after addition of one equivalent of Al^{3+} ion and now the quantum yield was calculated to be 0.037 and 0.039 for receptor R1and R2 respectively. In the absence of Al^{3+} ion, the receptors R1 and R2 displays bright blue

emission under the irradiation at long UV light, while addition of Al^{3+} ion, the emission was quenched and produces almost nil-fluorescence (Fig.7, Fig.8 insert).

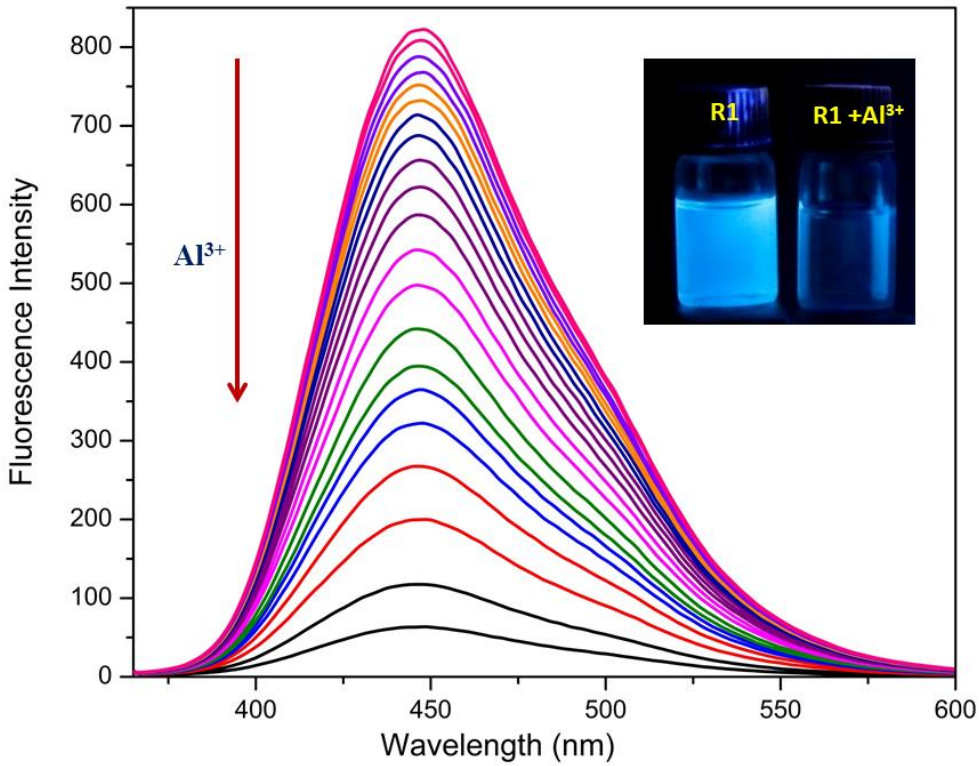

Fig.7. Fluorescence spectra of R1 with increasing concentration of Al^{3+} ion in HEPES buffer solution (20 mM HEPES), pH = 7.2, 50% (v/v; CH_3CN).

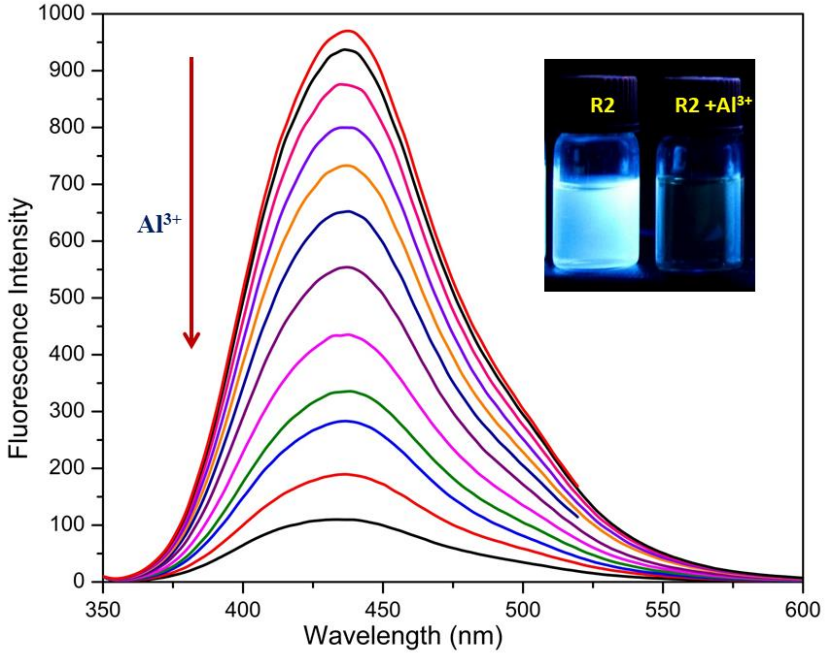

Fig.8. Fluorescence spectra of R2 with increasing concentration of Al^{3+} in HEPES buffer solution (20 mM HEPES), pH = 7.2, 50% (v/v) CH_3CN).

Competition experiment

To further investigate the competitive behavior of receptors R1 and R2 towards Al^{3+} ion with other coexist metal ions, the competitive experiment was carried out, the interference of coexist metal ions to Al^{3+} detection was investigated by fluorescence spectra as exhibited in Fig.9 and 10. Receptor R1 and R2 displays excellent selectivity for Al^{3+} ion over other tested metal ions. Additionally, competitive metal ions did not cause any significant changes in fluorescence intensity of receptor R1 and R2 in presence of Al^{3+} ion. These results suggested that receptor R1 and R2 could be used as Al^{3+} selective fluorescent turn-off chemosensor.

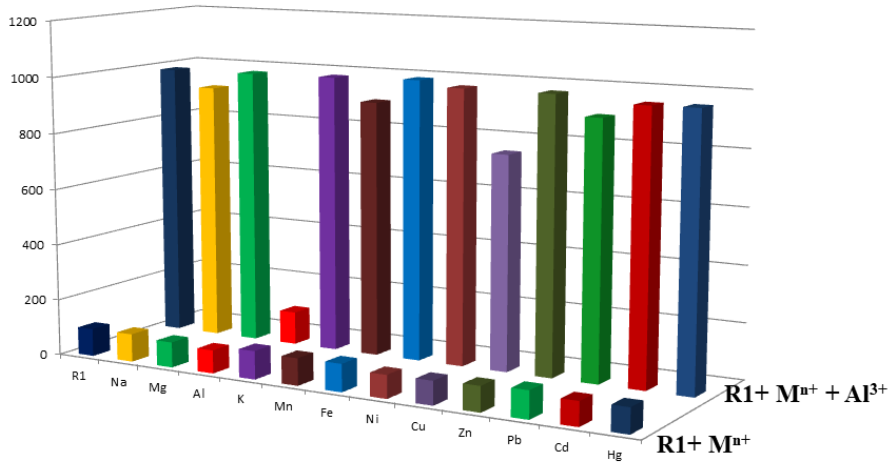

Fig. 9. Fluorescence intensity of R1 (10 μmol/L) to various metal ions. The first row represents intensity of R1 in the presence of 5 equiv. of various metal ions; the second row represents intensity of above solution upon addition of 5 equiv. of Al^{3+} ion.

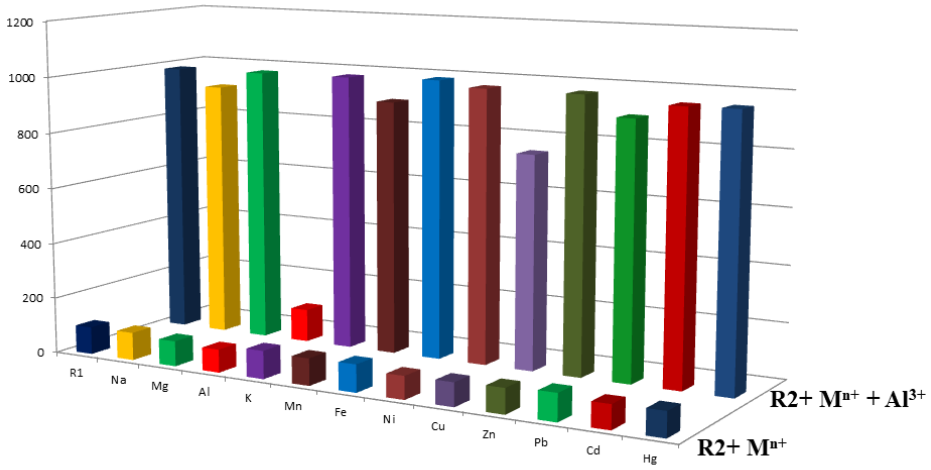

Fig. 10. Fluorescence intensity of R2 (10 μmol/L) to various metal ions. The first row represents intensity of R2 in the presence of 5 equiv. of various metal ions; the second row represents intensity of above solution upon addition of 5 equiv. of Al^{3+} ion.

. **Binding stoichiometry and association constant**

The stoichiometric behavior of receptors R1 and R2 towards Al^{3+} ion were determined by Job's plot method by measuring fluorescence intensity at different mole

fractions of Al^{3+} ion (0-1). The relative fluorescence intensity values was plotted against $[Al^{3+}]/ \{[Al^{3+}] +[R]\}$. A maximum emission was observed when molar fraction of Al^{3+} ion reached 0.5 (Fig.10 and Fig.S10) indicating that Al^{3+} ion form a 1:1 binding stoichiometry for $[R1\text{-}Al^{3+}]$ and $[R2\text{-}Al^{3+}]$. The association constant for formation of respective complexes $[R1\text{-}Al^{3+}]$ and $[R2\text{-}Al^{3+}]$ were estimated graphically by plotting $1/\Delta F$ against $1/[\ Al^{3+}\ ]$ (Fig.11 and S11). The data were linearly fitted to Benesi–Hildebrand equation and Ka values were obtained from slope of linear plot. The association constant for Al^{3+} ion binding in R1 and R2 were determined to be $1.84 \times 10^4\ M^{-1}$ and $1.92\times10^4\ M^{-1}$ respectively. Sensitivity of R1 and R2 towards Al^{3+} ion has been checked by determining limit of detection (LOD) value. By using the fluorescence titration results, the detection limits for Al^{3+} were found to be 8.92×10^{-8} M and 1.04×10^{-7} M on the basis of $3\sigma/m$ (Fig.S12 and Fig.S13). where σ is the standard deviation of the blank signals and m is the slope of the linear calibration plot (Fig. S6). According to World Health Organization (WHO) standard the concentration of Al^{3+} should be lower than 7.41 mM in drinking water [33, 34], which means that the sensors R1 and R2 are sensitive enough to monitor the water quality of drinking water. In Table S1† some recently reported chemosensors for selective detection of Al^{3+} ion has been described along with their LOD values. Those have some advantages over the others though it has some draw backs too. Our probe is synthesized by easy single step Schiff base condensation process. LOD value is significantly low but not the lowest among all reported.

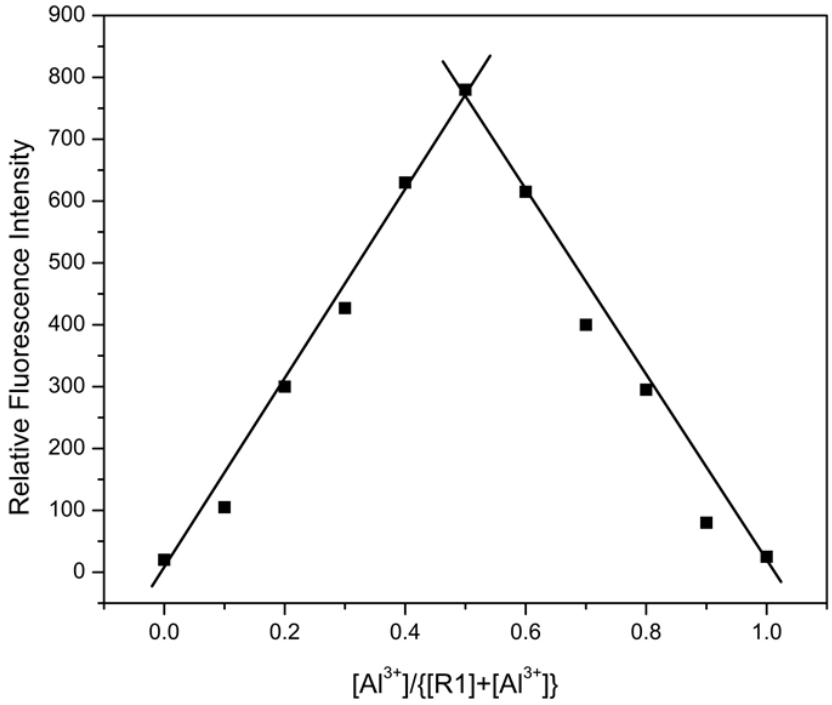

Fig. 11. Job plot for 1:1 complex of R1 and Al^{3+} ion at 447 nm.

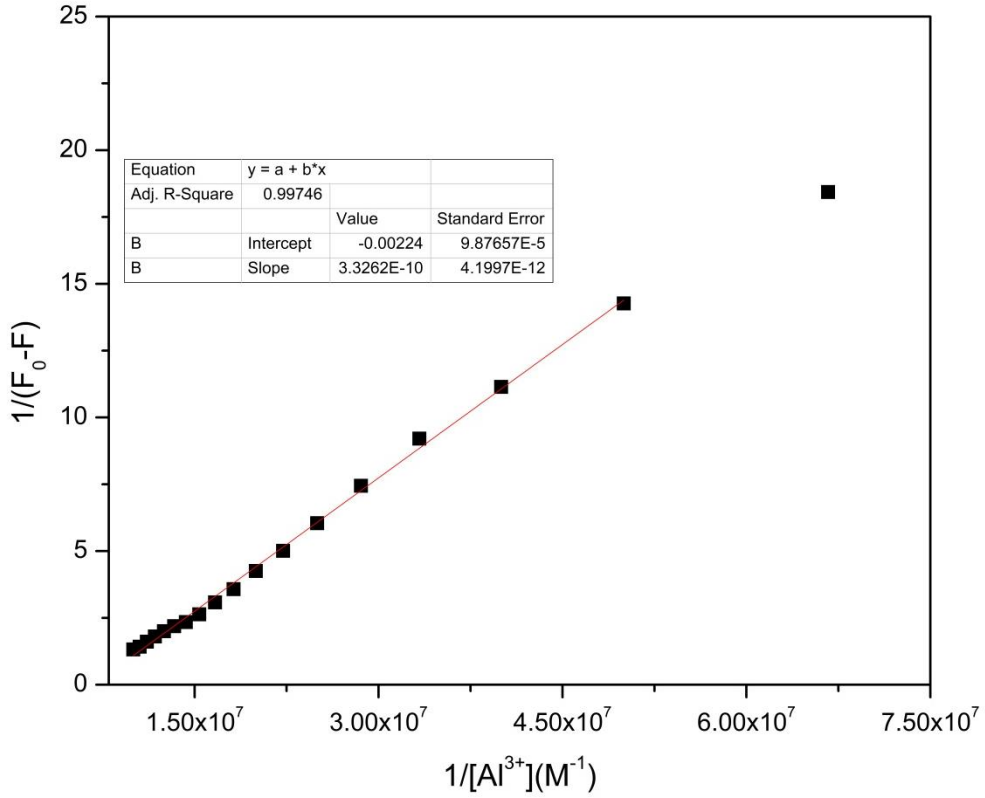

Fig. 12. Benesi–Hildebrand plot (at 447nm) for complexation of R1 with Al^{3+} ion.

Conclusion

Thiophene and furan appended pyrazoline based receptors R1 and R2 have been synthesized and their photophysical properties examined by UV-visible and fluorescence spectrophotometers. The receptors R1 and R2 demonstrate an excellent selective and sensitive response to Al^{3+} ion over other metal ions. Among them, receptor R1 exhibit absorption and emission bond centered at longer wavelength and high fluorescence intensity compared to receptor R2. The fluorescence nature of receptors gradually decreased upon the addition of Al^{3+} ion. The chemosensor R1 and R2 displayed a 1:1 complex formation with Al^{3+} ion with an association constant of 1.84×10^4 M^{-1} and 1.92×10^4 M^{-1} respectively. Both probes have good detection limits for Al^{3+} ions since 8.92×10^{-8} M (R1) and 1.04×10^{-7} M (R2). Receptors R1 and R2 can be used as selective 'Turn-Off' sensor for Al^{3+} ion.

Acknowledgements:

The author R.M. thanks the Anna Centenary Research Fellowship (ACRF), Anna University, Chennai (CR/ACRF/2013/38) for financial support. P.K. is thankful to UGC, New Delhi for the award of UGC-BSR Faculty Fellowship [F.18-1/2011(BSR) dated 30.12.2016]. Instrumentation facility provided under FIST-DST and UGC-DRS to Department of Chemistry, Anna University are sincerely acknowledged.

Appendix A. Supplementary data

Characterization data and additional spectroscopic data are available as supplementary data.

References:

[1] S. O. Aderinto, Y. Xu, H. Peng, F. Wang, H. Wu, X. Fan, J Fluoresc. 2 (2017) 79-87.

[2] S. R. Patil, J. P. Nandre, P. A. Patil, S. Bothra, S. K. Sahoo, A. Klásek, U. D. Patil, Inorg. Chem. Commun. 49 (2014) 59-62.

[3] Y. J. Na, I. H. Hwang, H. Y. Jo, S. A. Lee, G. J. Park, C. Kim, Inorg. Chem. Commun.35 (2013) 342-345.

[4] G. Y. Yeap, E. Hrishikesan, Y. H. Chan, W. A. K. Mahmood, J Fluoresc. 27 (2017) 105-110.

[5] H. Wang, Y. Li, S. Xu, Y. Li, C. Zhou, X. Fei, X. Xu, Org biomol chem. 9 (2011) 2850-2855.

[6] E. Hrishikesan, C. Saravanan, P. Kannan, Ind. Eng. Chem. Res. 50 (2011) 8225-8229.

[7]. C Marín-Hernández, L. E. Santos-Figueroa, S El Sayed, T Pardo, M M M Raposo, R M Batista, R Martínez-Máñez, Dyes and Pigments. 122 (2015) 50-58.

[8]. C Marin-Hernandez, L E Santos-Figueroa, M E Moragues, M M M Raposo, R M Batista, S P Costa, F Sancenon, The Journal of organic chemistry. 79 (2014) 10752-10761.

[9] S. A. Lee, G. R. You, Y. W. Choi, H. Y. Jo, A. R. Kim, I.Noh, , C. Kim, Dalton Transactions. 43 (2014) 6650-6659.

[10] S. Kim, J. Y. Noh, K. Y. Kim, J. H. Kim, H. K. Kang, S. W. Nam, J. Kim, Inorganic chemistry. 51 (2012) 3597-3602.

[11] R., Azadbakht, M., Talebi, J., Karimi, R. Golbedaghi, Inorg. Chim. Acta. 453 (2016) 728 - 734.

[12] M. I. Yousef, A. M. El-Morsy, M. S. Hassan, Toxicology. 215 (2005) 97-107.

[13] D. P. Perl, A. R. Brody, Science. 208 (1980) 297-299.

[14] D. P. Perl, D. C. Gajdusek, R. M. Garruto, R. T. Yanagihara, C. J. Gibbs, Science. 217 (1982) 1053-1055.

[15] J R Walton, (2007) J. Inorg Biochem. 101: 1275-1284.

[16] E. Altschuler, Med. hypotheses. 53 (1999) 22-23.

[17] B. Wang, W Xing, Y Zhao, X Deng, Environ. Toxicol. Pharmacol. 29 (2010) 308-313.

[18] E. Delhaize, P. R. Ryan, Plant. Physiol. 107 (1995) 315–321.

[19] T. Guray, Ü. D. Uysal, T. Gedikbey, A. A. Huseyinli, Anal. Chim. Acta. 545 (2005) 107-112.

[20] I. Narin, M. Tuzen, M. Soylak, Talanta. 63 (2004) 411-418.

[21] H. Wang, Z. Yu, Z. Wang, H. Hao, Y. Chen, P. Wan, Electroanalysis. 23 (2011) 1095-1099.

[22] X. Xie, Y. Qin, Sensors and Actuators B: Chemical, 156 (2011) 213-217.

[23] (a) R. Manjunath, E. Hrishikesan, P. Kannan, Spectrochim. Acta A. 140 (2015) 509-515. (b). E. Hrishikesan, R. Manjunath, P. Kannan, J. Sol. Chem. 45 (2016) 907-919.

[24] R. Manjunath, P. Kannan, Opt. Mat. 79 (2018) 38-44.

[25] D.D. Perrin, W.L.F. Armarego, Purification of Laboratory Chemicals, third ed.,Pergamon press, New York, 1988

[26] A. Hasan, K. M. Khan, M. Sher, G. M. Maharvi, S. A. Nawaz, M. I. Choudhary, C. T. Supuran, J. Enzym. Inhib. Med. Chem. 20 (2005) 41-44.

[27] A. Budakoti, A. R. Bhat, A. Azam, Eur. J. Med. Chem. 44 (2009) 1317-1325.

[28] P. MacCarthy, Anal. Chem 50 (1978) 2165.

[29] H. A. Benesi, J. H. J. Hildebrand, J. Am. Chem. Soc. 71(1949) 2703–2707.

[30] R.A. Velapoldi, K.D. Mielenz. A Fluorescence Standard Reference Material: Quinine Sulfate Dihydrate. National Bureau of Standards (Now, The National Institute of Standards and Technology, NIST) Special Publication, Washington DC, US, (1980) pp. 260–264.

[31] S. Gao, L. Hao, J. Li, P. Lin, D. Li, S. Shuang, C. Dong, Luminescence. 28. (2013) 412-418.

[32] X H Zhang, S K Wu, Z Q Gao, C S Lee, S. T Lee, H L Kwong, Thin Solid Films. 371 (2000) 40-46.

[33]. Z. Krejpcio, R. W. Wojciak, Pol. J. Environ. Stud. 11 (2002) 251–254.

[34]. D.H. Kim, Y.S. Im, H. Kim, C. Kim, Inorg. Chem. Commun. 45 (2014) 15–19.

Graphical Abstract

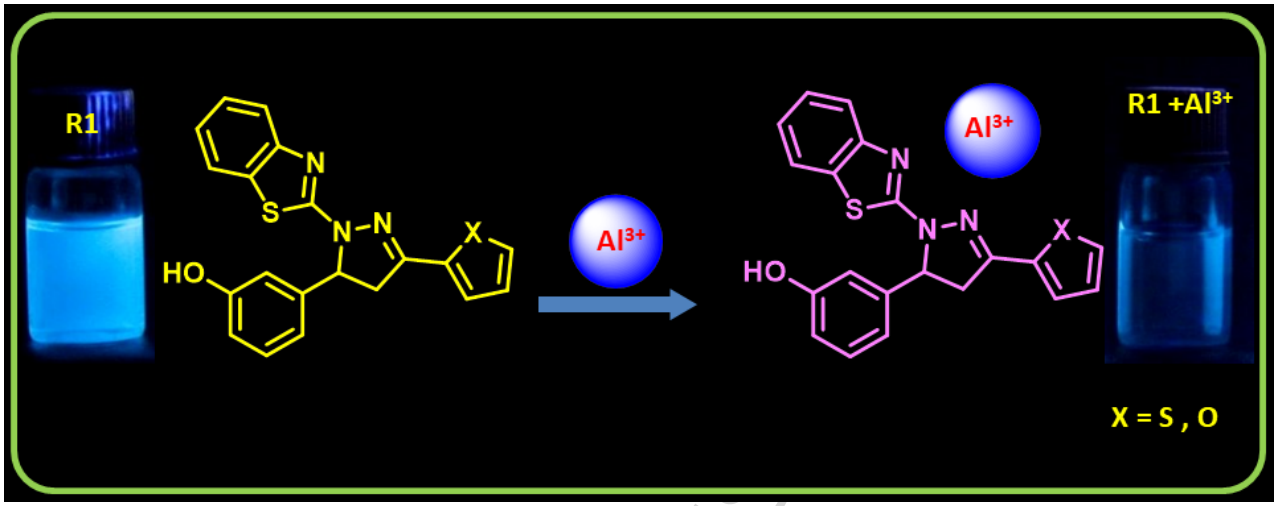

Highlights

- A selective fluorescent chemosensor for Al^{3+} was synthesized.
- The receptors **R1** and **R2** were displays an excellent selective and sensitive response to Al^{3+} ion over other metal ions.
- Job's plot indicated 1:1 binding- stoichiometry for receptor **R1** and **R2** with Al^{3+} ion.
- Association constant of receptor **R1** and **R2** with Al^{3+} is determined on the basis of Bensi-Hilderbrand as $K_a = 1.84 \times 10^4\ M^{-1}$ and $K_a = 1.92 \times 10^4\ M^{-1}$ respectively.
- The thiophene based receptor R1 exhibit high intensity absorption and emission bond at longer wavelength compered to furan based receptor R2.

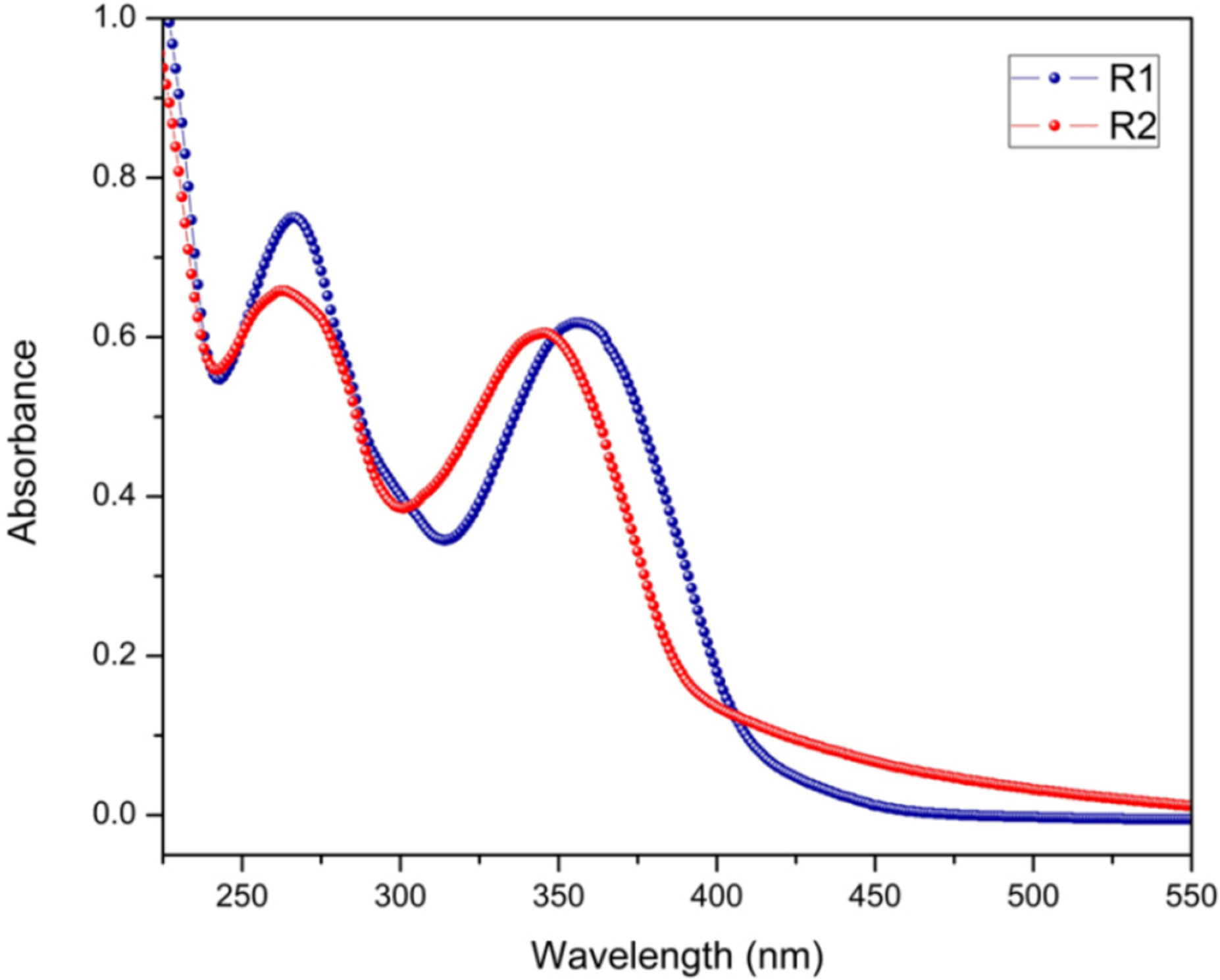
1.0
0.8
0.6
0.4
0.2
0.0
Absorbance
250
300
350
400
450
500
550
Wavelength (nm)
R1
R2

Figure 1

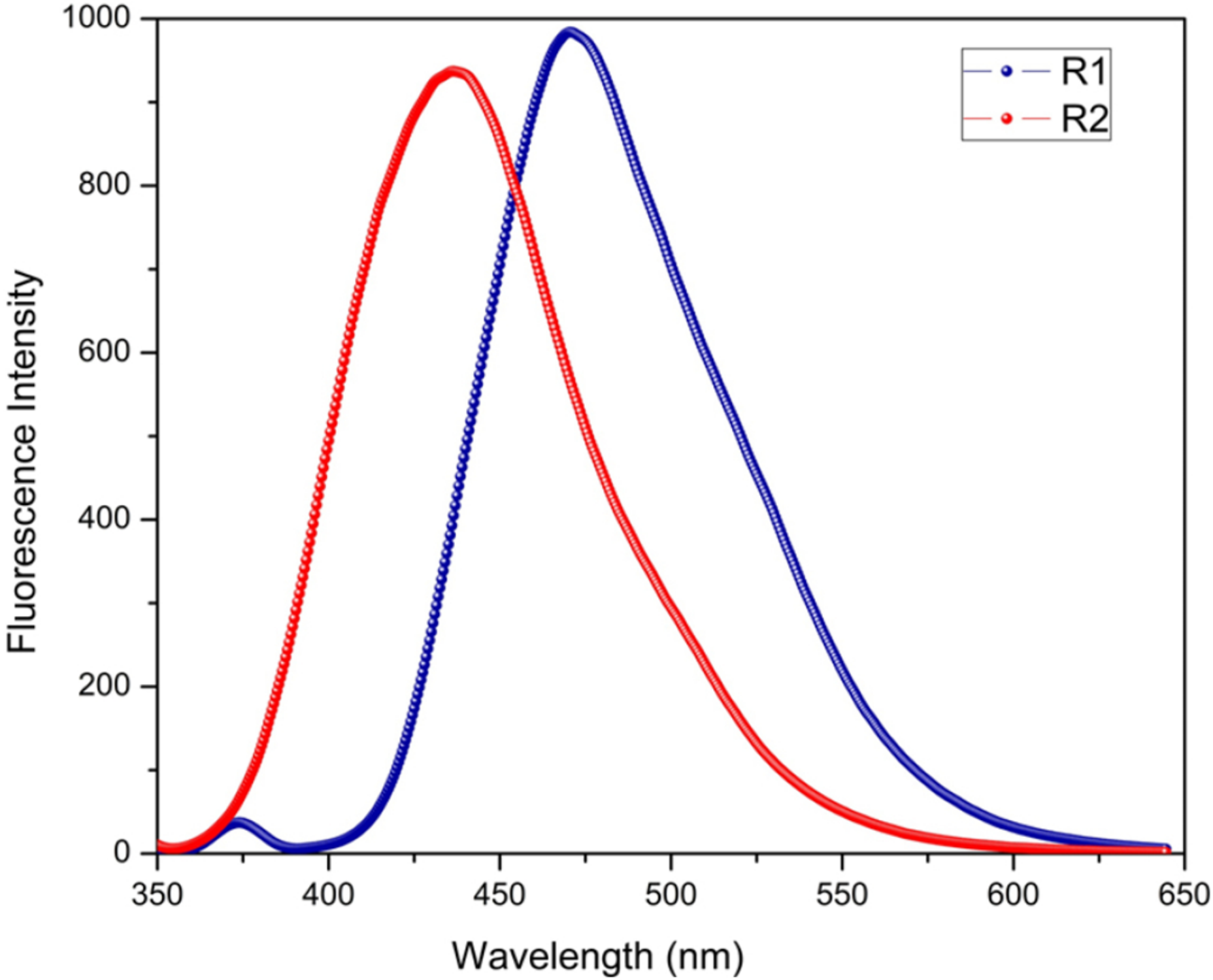
1000
800
600
400
200
0
Fluorescence Intensity
350
400
450
500
550
600
650
Wavelength (nm)
R1
R2

Figure 2

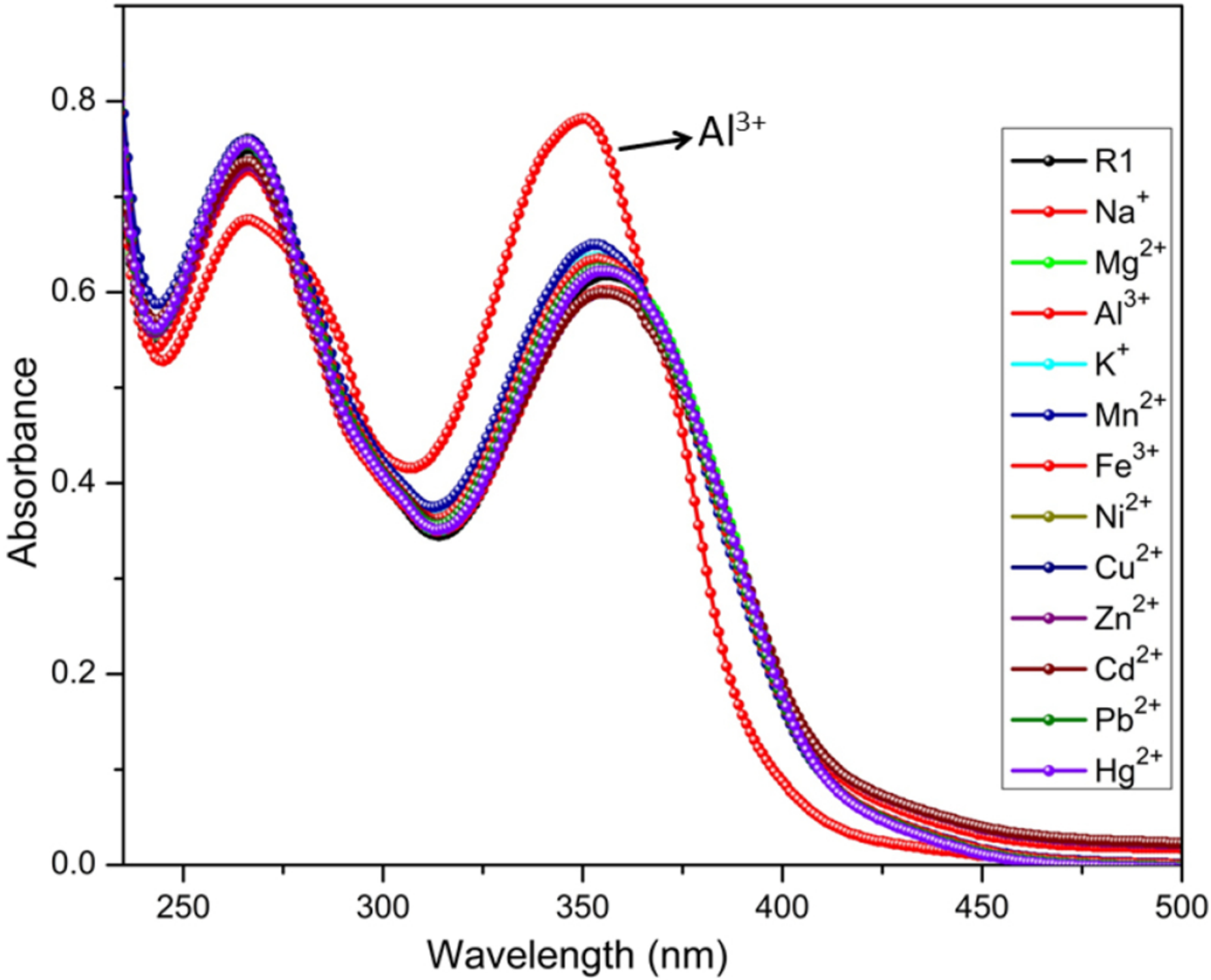
Absorbance
Wavelength (nm)
0.0
0.2
0.4
0.6
0.8
250
300
350
400
450
500
Al^{3+}
R1
Na^{+}
Mg^{2+}
Al^{3+}
K^{+}
Mn^{2+}
Fe^{3+}
Ni^{2+}
Cu^{2+}
Zn^{2+}
Cd^{2+}
Pb^{2+}
Hg^{2+}

Figure 3

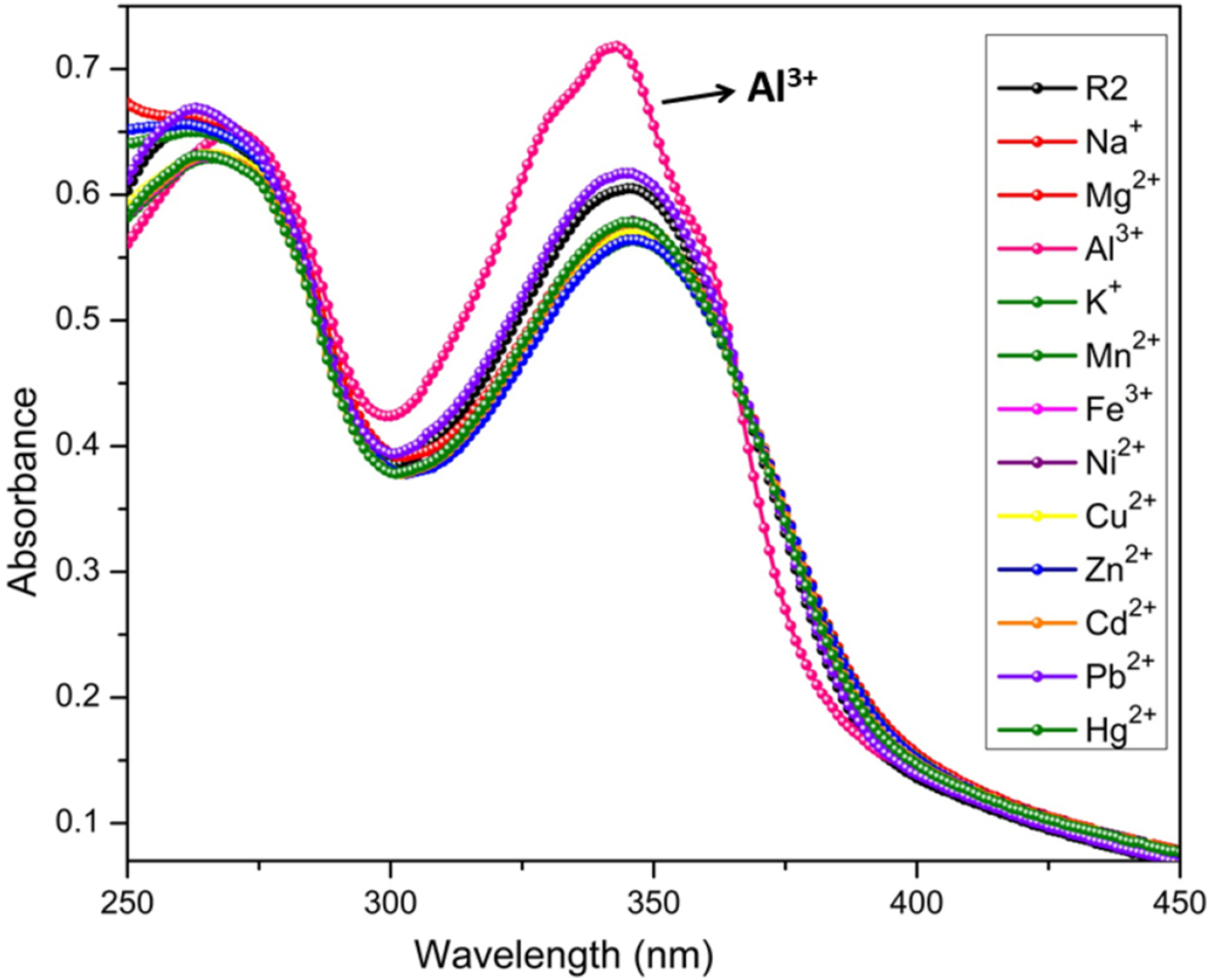
Absorbance
Wavelength (nm)
0.1
0.2
0.3
0.4
0.5
0.6
0.7
250
300
350
400
450
Al3+
R2
Na+
Mg2+
Al3+
K+
Mn2+
Fe3+
Ni2+
Cu2+
Zn2+
Cd2+
Pb2+
Hg2+

Figure 4

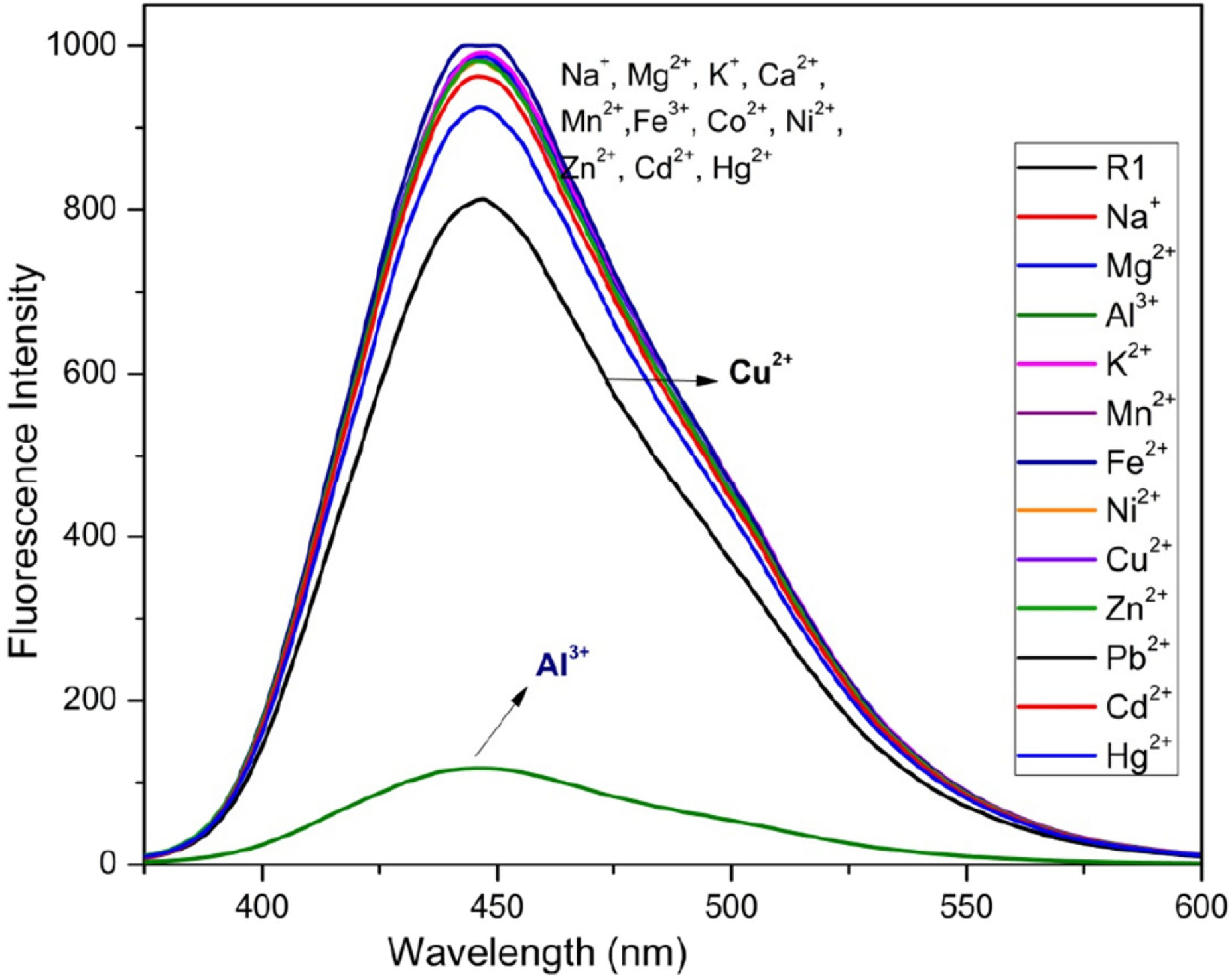
Fluorescence Intensity
Wavelength (nm)
1000
800
600
400
200
0
400
450
500
550
600
Na+, Mg2+, K+, Ca2+,
Mn2+,Fe3+, Co2+, Ni2+,
Zn2+, Cd2+, Hg2+
Cu2+
Al3+
R1
Na+
Mg2+
Al3+
K2+
Mn2+
Fe2+
Ni2+
Cu2+
Zn2+
Pb2+
Cd2+
Hg2+

Figure 5

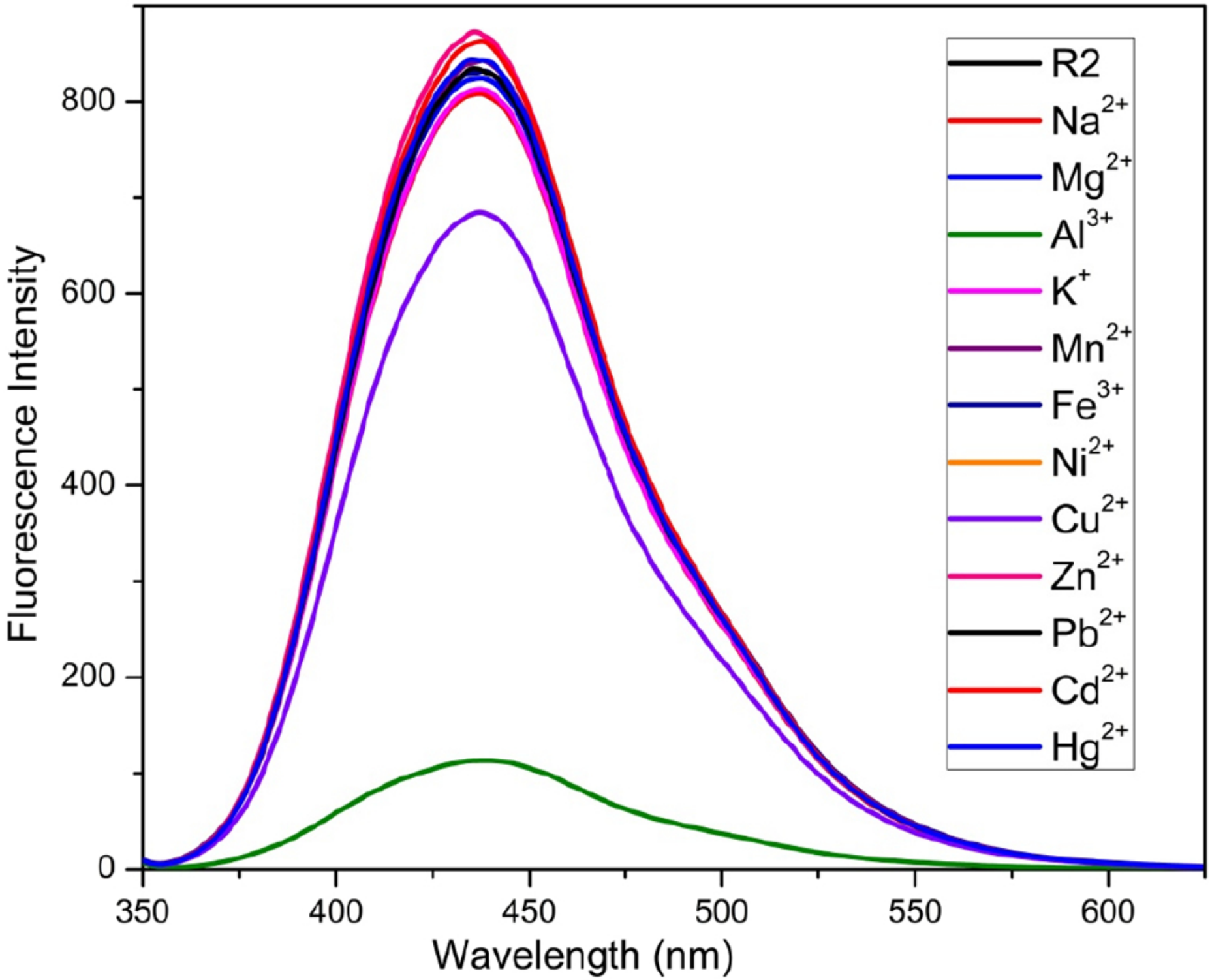
Fluorescence Intensity
0
200
400
600
800
350
400
450
500
550
600
Wavelength (nm)
R2
Na2+
Mg2+
Al3+
K+
Mn2+
Fe3+
Ni2+
Cu2+
Zn2+
Pb2+
Cd2+
Hg2+

Figure 6

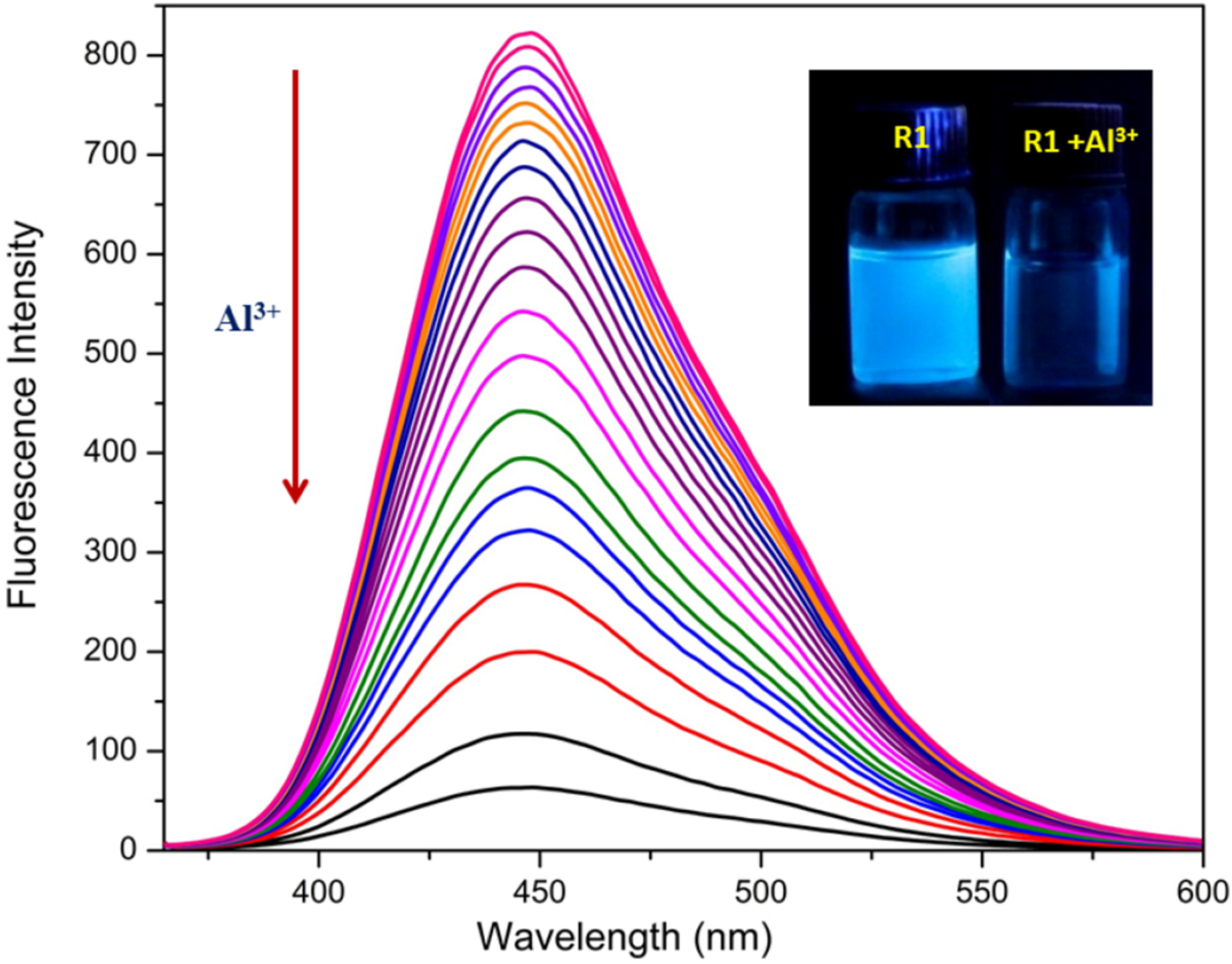
Fluorescence Intensity
Wavelength (nm)
Al3+
R1
R1 +Al3+
0
100
200
300
400
500
600
700
800
400
450
500
550
600

Figure 7

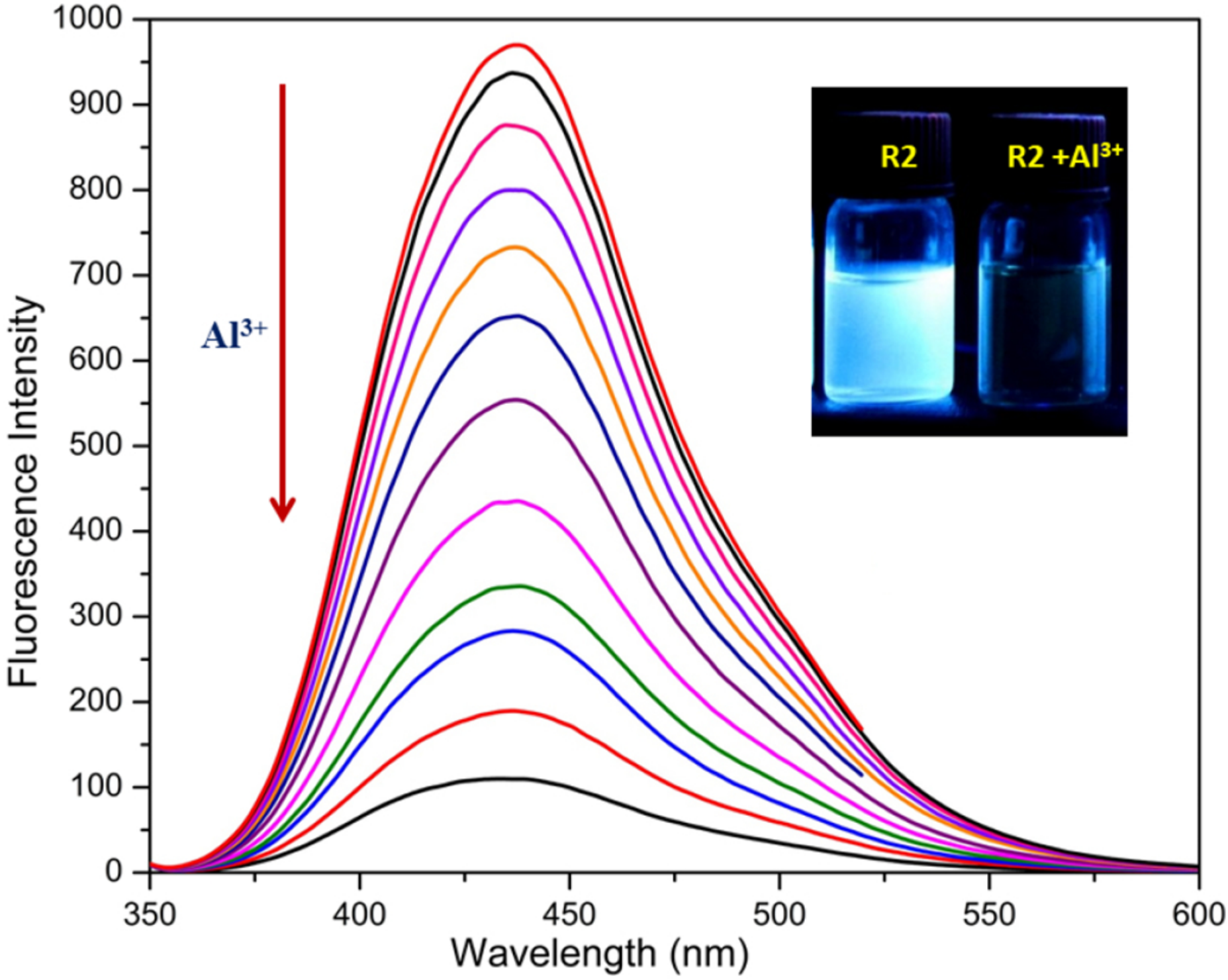
Fluorescence Intensity
Wavelength (nm)
Al3+
R2
R2 +Al3+
0
100
200
300
400
500
600
700
800
900
1000
350
400
450
500
550
600

Figure 8

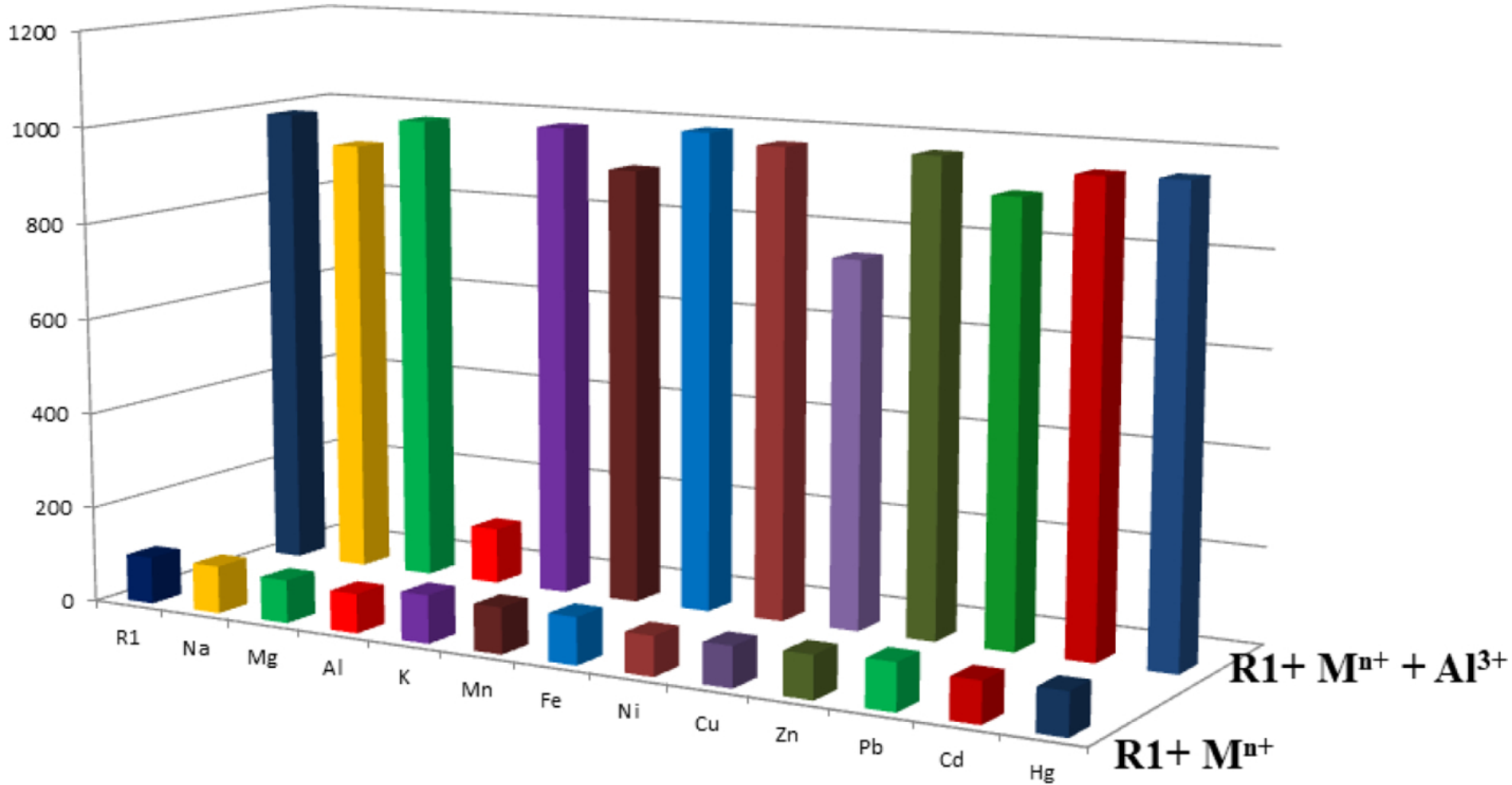
1200
1000
800
600
400
200
0
R1
Na
Mg
Al
K
Mn
Fe
Ni
Cu
Zn
Pb
Cd
Hg
R1+ Mⁿ⁺ + Al³⁺
R1+ Mⁿ⁺

Figure 9

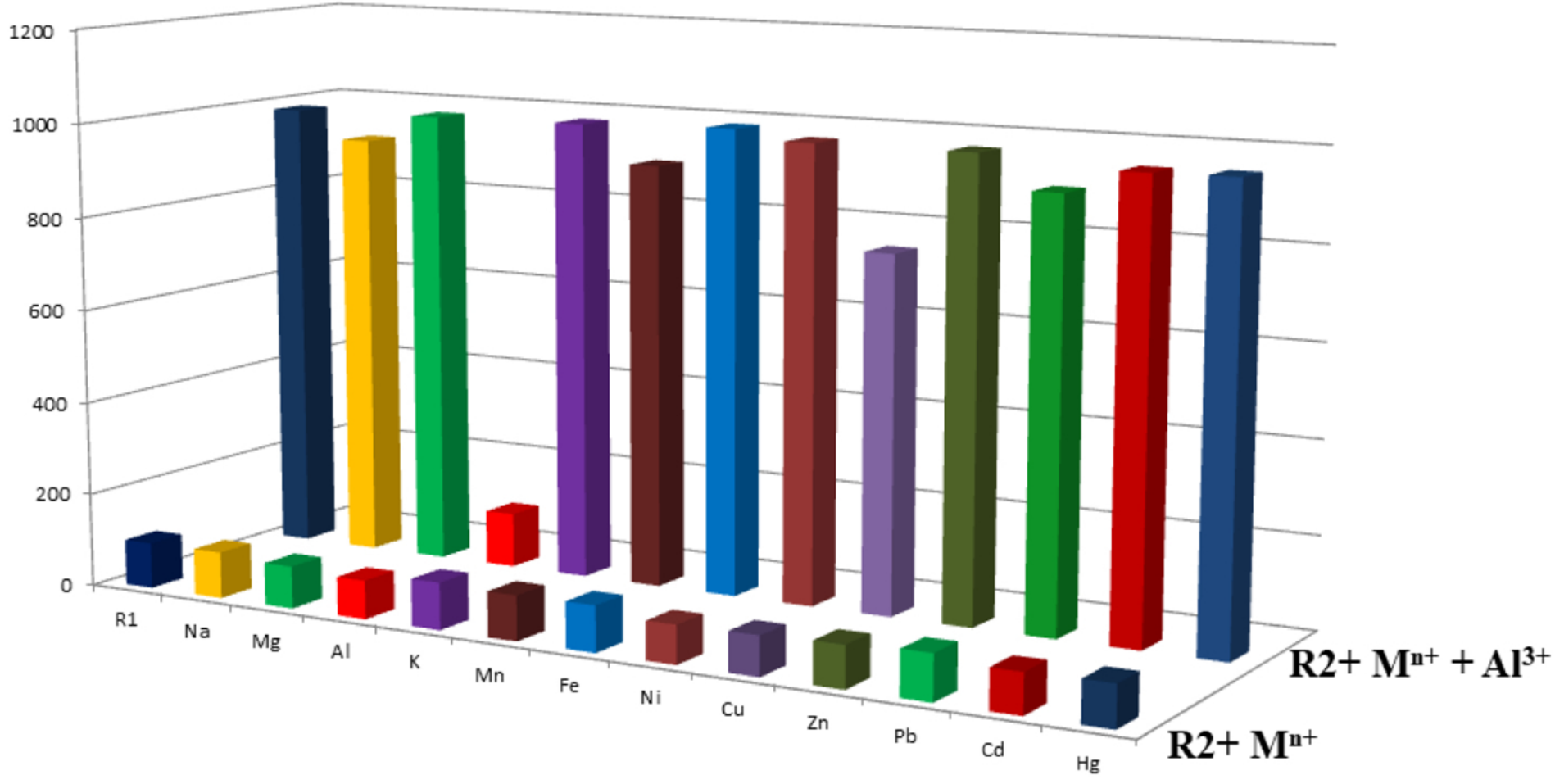
1200
1000
800
600
400
200
0
R1
Na
Mg
Al
K
Mn
Fe
Ni
Cu
Zn
Pb
Cd
Hg
R2+ Mⁿ⁺ + Al³⁺
R2+ Mⁿ⁺

Figure 10

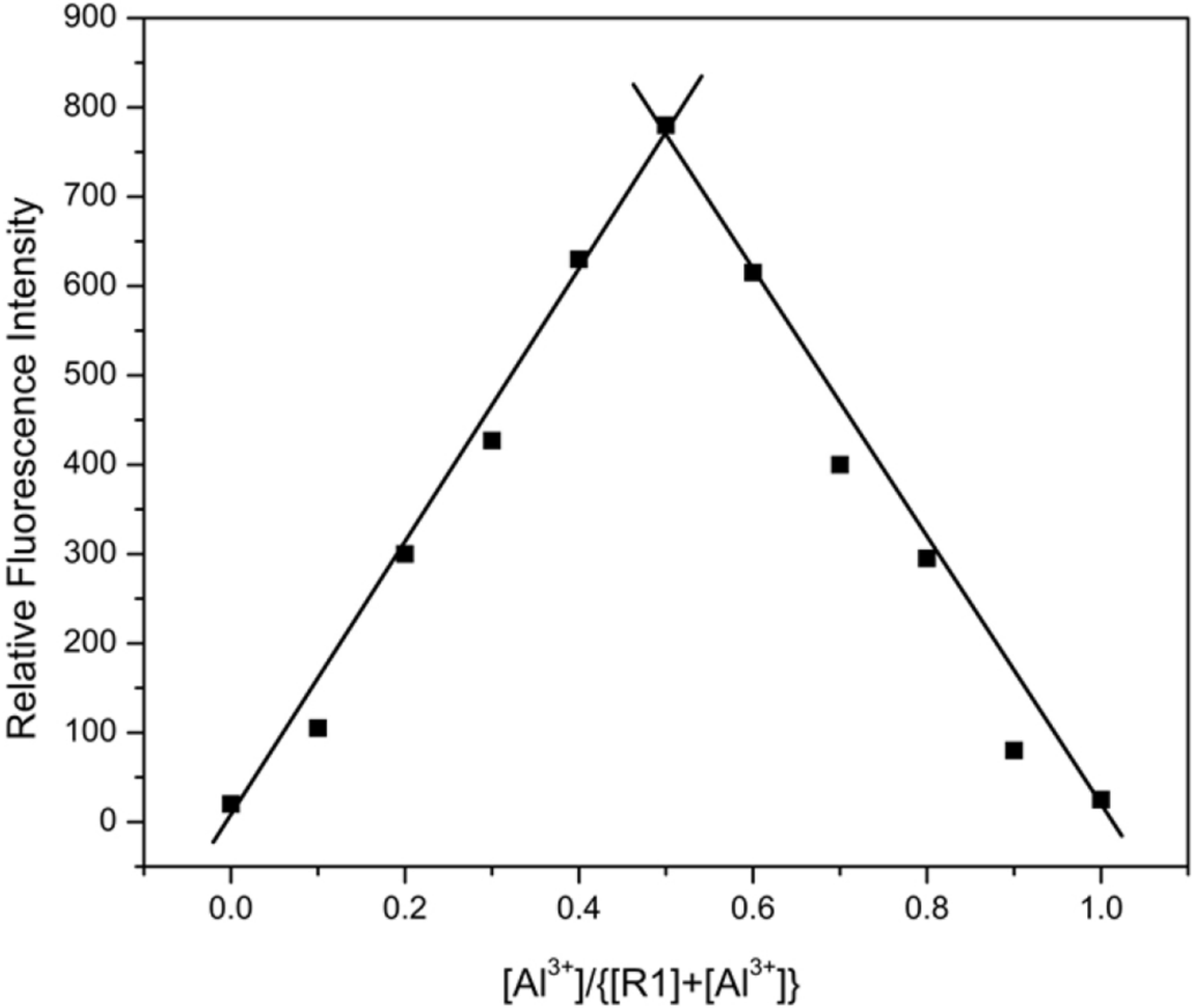
900
800
700
600
500
400
300
200
100
0
Relative Fluorescence Intensity
0.0
0.2
0.4
0.6
0.8
1.0
[Al3+]/{[R1]+[Al3+]}

Figure 11

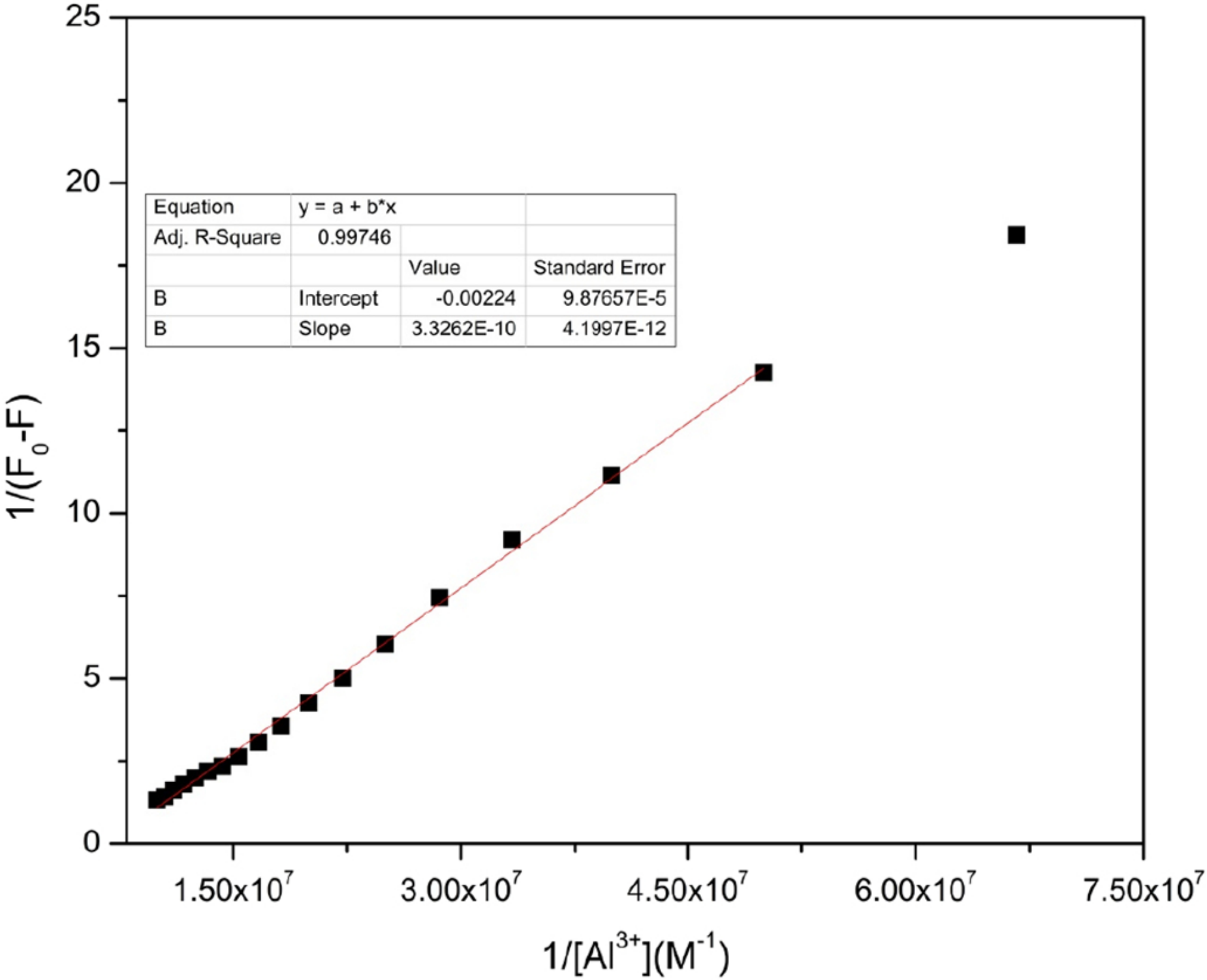
Equation y = a + b*x
Adj. R-Square 0.99746
Value Standard Error
B Intercept -0.00224 9.87657E-5
B Slope 3.3262E-10 4.1997E-12
25
20
15
10
5
0
1/(F0-F)
1.50x10^7
3.00x10^7
4.50x10^7
6.00x10^7
7.50x10^7
1/[Al3+](M-1)

Figure 12